Comprehensive Design and Experimental Verification of Shunt Active Power Filter

Mohammad Pichan
Department of Electrical Engineering
Arak University of Technology
Arak, Iran
m.pichan@arakut.ac.ir

Hossein Hafezi
Faculty of Information Technology and Communications
Tampere University
Tampere, Finland
hossein.hafezi@tuni.fi

Hikmat Basnet
Faculty of Information Technology and Communications
Tampere University
Tampere, Finland
hikmat.basnet@tuni.fi

Tomi Roinila
Faculty of Information Technology and Communications
Tampere University
Tampere, Finland
tomi.roinila@tuni.fi

Abstract—**Harmonic pollution imposed by non-linear loads has become one of the main power quality challenges. In addition, reactive power absorption related to non-linear loads may result in serious power quality issues like voltage drop or voltage instability. Among different passive and active power filters (APFs), shunt active power filter (SAPF) is used a lot since it can compensate both complete harmonic and reactive components as well as high flexibility without any resonance. However, harmonic detection, hardware, and control design play vital role in the performance of the SAPF. From hardware point of view, design of the DC-link capacitor and series inductor are two main challenges. In this paper, a comprehensive design procedure is presented to design the suitable passive elements. In addition, high performance control design is also considered. Several simulation and experimental results are provided to verify the proper design and controller performance.**

Keywords—Shunt Active Power Filter, Passive component design, Harmonic current components

I. INTRODUCTION

Nowadays, the power electronics-based devices have experienced a fast growth because of advancement in power electronics and semiconductor technologies [1,2]. However, they act as a non-linear load to the grid causing power quality issues. In addition, reactive power absorption related to non-linear loads may result in serious power quality issues like voltage drop or voltage instability [3]. Hence, harmonic and reactive power compensation of such a non-linear load is important [4]. So far these issues have been addressed using passive or active filters. The idea of passive method is using RLC filters to compensate harmonics. However, using these filters only a specific harmonic can be eliminated. Moreover, these filters suffer from reactive power injection, probable resonance, and irrelevant compensation [5].

To overcome these issues, active power filters (APF) have been proposed with the idea of using power switches along with the passive filters [6]. Active power filter structures can be divided to series, shunt, or hybrid configurations. Shunt active power filters compensates current harmonics and are widely used in industrial applications. This structure can provide complete harmonic compensation and controllable reactive power injection. In addition, it offers high flexibility without any resonance [7].

In this paper, two vital issues in shunt active power filters have been addressed: design of passive components and control system. From hardware point of view, design of the input DC capacitor and series inductor can be considered as the main challenges. The input capacitor is responsible for maintaining a constant DC voltage which is necessary to generate reactive power. On the other hand, the inductor value affects current generation ability as well as current ripple. It is worth mentioning that under fast load current changes, the APF should be able to make high current deviation which is directly proportional to the inductor value. However, low inductor value results in high frequency current ripple, which is transferred to the grid. Consequently, precise design of hardware elements of APF is very critical issue.

The control system plays a vital role in an electrical system, and it is even more critical in APFs since a non-sinusoidal current must be generated. From control point of view, fast detection beside simultaneous harmonic generation is vital for a better APF performance. Steady state error of the system is another important issue, which directly affects the APF performance. As a result, different control methods have been proposed to control the APFs such as direct power control (DPC), which has the advantages of easy implementation and fast dynamic response [8,9]. However, the conventional DPC suffers from high sampling frequency and variable switching frequency, which makes the design of the filter and the cooling system demanding and complex [10]. Thus, constant switching frequency is obtained using predictive direct power control (P-DPC) [11] and DPC with space vector modulation (DPC-SVM) [12]. Nevertheless, P-DPC needs complex calculations and DPC-SVM requires coordinate transformation and exact tuning of PI gains to prevent a power overshoot [8]. The methods such as dead-beat control [13,14], sliding mode control [15,16], and predictive control [17] have also shown good dynamic response. However, dead-beat controller suffers from steady state error, sliding mode control has a complex design and implementation, whereas predictive control suffers from steady state error and high computational burden. Nevertheless, multi-resonant controller can overcome these

problems by offering simplicity in design and implementation, reducing the steady-state error [18, 19]. In order to achieve the targets of this controller, the optimum design of control parameters must be addressed.

This paper presents a comprehensive yet simple design of hardware elements and implements a multi-resonant control system for APF operation. The feasibility and performance of the proposed design is validated through experimental results using a non-linear load.

The remainder of the paper is organized as follows. Section II provides the comprehensive design of passive elements. Section III presents the proposed control system. Section IV shows the simulation results and its experimental verification. Finally, section V concludes the paper.

II. Passive Element Design

According to the hardware structure of the SAPF depicted in Fig. 1, design of the DC-Link capacitor as well as series inductor are two main challenges.

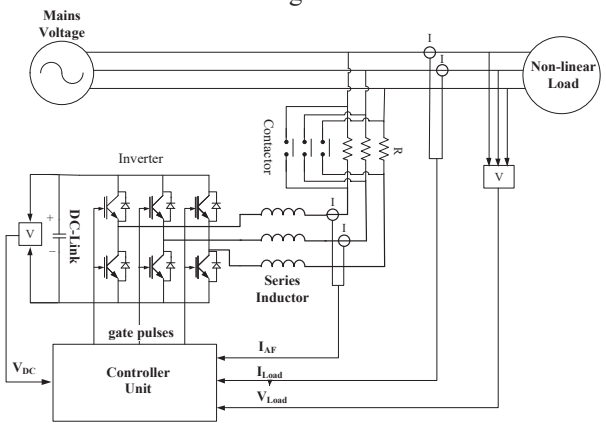

Fig. 1. The structure of SAPF.

A. DC-link Capacitor Design

The DC-link capacitor is responsible for maintaining a constant DC voltage and generate reactive power. Capacitor selected with small value increases the ripple in the DC-link voltage. This voltage ripple deteriorates the control performance by generating additional harmonic in to the injected SAPF current. On the other hand, large capacitor value will reduce the DC-link voltage ripple significantly. However, larger value results in higher size, weight, cost, and poor dynamic response. Hence, appropriate sizing of DC-link capacitor is important.

There are several approaches to select the proper capacitor value. It can be based on rigorous calculation of RMS DC-link current [20]. Capacitor value can also be selected based on maximum energy demand during transient, or peak voltage ripple, or harmonic current [21]. However, a simple method, on the basis of currents in each leg, is proposed in this paper. Thus, the current of the DC-link capacitor can be written as:

$$i_{dc} = s_1 i_1 + s_2 i_2 + s_3 i_3 \tag{1}$$

where i_1, i_2 and i_3 are the currents in each leg of the inverter. Whereas S_k is the switching state of each leg defined as follow:

$$s_k = \begin{cases} 1 & upper\ switch\ ON,\ lower\ switch\ OFF \\ 0 & upper\ switch\ OFF,\ lower\ switch\ ON \end{cases} \tag{2}$$

Among several PWM methods, space vector modulation (SVM) technique is considered as one of the best modulation techniques. There are eight possible switching vectors including six active and two zero vectors. The reference voltage vector is produced with two active and two zero vectors in each sector. Also, the volt-second balance is maintained by calculating suitable application for these vectors. Then, the application time for each active and zero vectors are defined as:

$$\begin{aligned} t_1 &= m\sqrt{3}\frac{T_{sw}}{2} sin\left(\frac{\pi}{3} - wt\right) \\ t_2 &= m\sqrt{3}\frac{T_{sw}}{2} sin(wt) \\ t_0 &= \frac{T_{sw}}{2} - (t_1 + t_2) = \frac{T_{sw}}{2}\left[1 - \sqrt{3} m sin\left(\frac{\pi}{3} + wt\right)\right] \end{aligned} \tag{3}$$

where m and T_{sw} are modulation index and switching time, respectively. The capacitor current involving high frequency components, which results in a constant DC voltage in addition to the voltage ripple, is given as:

$$V_{de}(t) = V_{DC} + \Delta V_{dc}(t) \tag{4}$$

To determine $\Delta V_{dc}(t)$, it is worth to be mentioned that the whole i_{dc} flows through the capacitor. Hence, ΔV_{dc} can be calculated by integrating i_{dc} over a specific time interval t_{pp} as:

$$\Delta V_{pp} = \left|\frac{1}{C}\int_0^{t_{pp}} V_{de}(t)\,dt\right| \cong \frac{1}{C}|\Delta I|\,t_{pp} \tag{5}$$

where current ripple ΔI and t_{pp} are related to factors such as m and ωt. Based on (5) and SVM equations, the capacitor value can be calculated as (6).

$$C \geq \frac{1}{4 f_{sw}} \frac{I_o}{\Delta V_{pp}^{\ max}} \tag{6}$$

where f_{sw} is the switching frequency, I_o is the maximum SAPF phase current whose value is related to the load current, and $\Delta V_{pp}^{\ max}$ is the maximum acceptable ripple voltage. If SAPF is used to only compensate the current harmonics, it is about 35-50% of the load peak current. On the other hand, if SAPF is used to compensate both harmonics and reactive components, it is about 50-70% of load peak current. Another issue related to the capacitor is the DC voltage and maximum acceptable $\Delta V_{pp}^{\ max}$. The DC-link voltage is usually selected on the basis of the peak line voltage as:

$$V_{dc} = 1.25 * \frac{V_{1-peak}}{m_{\max}} \tag{7}$$

where m_{max} is the maximum permitted modulation index which is mainly related to the deadtime of each leg switches. Usually, $\Delta V_{pp}^{\ max}$ is considered about 2-4% of the DC-Link

voltage. Hence, an appropriate DC-Link capacitor value can be calculated.

B. Inductor Filter Design

High frequency switching performance of SAPF results in switching current harmonic and ripple. Since the SAPF is connected to the Point of Common Coupling (PCC), these harmonics will be injected to the grid current which deteriorates the grid voltage and current quality. To prevent these harmonics from transferring to the grid, a lowpass filter is used in the SAPF output. Usually, series inductor filter is used to reduce and attenuate the switching current harmonics. Large inductor value will highly attenuate the current harmonics but, the dynamic response of SAPF in current harmonic injection is reduced, considerably. It is worth to be mentioned that the rate of current change of inductor filter (di/dt) is proportional to the effective voltage across the inductor and it is inversely proportional to the inductor value. Therefore, large inductor value is not suitable for SAPF applications.

The inductor value can be selected on the basis of harmonic content, or peak ripple current, or peak to peak inductor current [21]. The inductor value is mainly related to the applied DC voltage (V_{DC}), switching frequency (f_{sw}) and maximum permitted ripple current ($\Delta i_{L,\,max}$). Hence, a simple and efficient procedure is to select the filter inductor based on (8):

$$L = \frac{V_{DC}}{8 f_{sw} \Delta i_{L,\,max}} \tag{8}$$

As mentioned before, high ripple current will deteriorate the grid current quality. Hence, the maximum permitted ripple current is usually as low as 10-15% peak inductor current. This value will satisfy both low ripple current and high dynamic response.

III. CONTROL SYSTEM

The control system of SAPF consists of two parts: 1- harmonic detection part, 2- harmonic generation part. For three phase three-wire systems, PQ power theory is the most beneficial one in which, the grid harmonic components are related to the ripples in active and reactive power. Fig. 2 shows the control strategy for harmonic detection based on PQ power theory. The outer loop voltage regulator is responsible to maintain a constant DC-link voltage and provide reference current component in d-axis. The grid voltage U_{abc} provides the phase angle θ through a phase locked loop. This phase angle θ is used in park transformation of the load current i_{abc}. The load current in dq-axis is added to the reference current generated by the DC voltage regulator. Applying inverse park transformation provides a three-phase APF current reference.

Although precise harmonic detection can highly affect the SAPF performance, the control system which is responsible for harmonic generation should be selected and designed carefully. The SAPF should compensate current harmonics with different frequency. On the other hand, precise harmonic tracking as well as high dynamic response under rapid load changes is important. The same as PI controllers for DC control signals. Proportional Resonant (PR) controller can

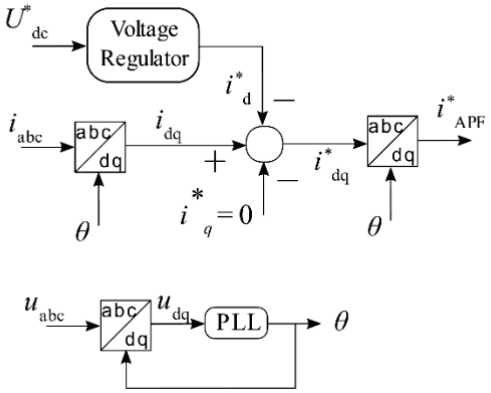

Fig. 2. Outer control loop of APF for harmonic detection.

provide zero steady-state error at designed central frequency (ω_n).

$$G_R = \frac{K_R S}{S^2 + 2\xi^5 w_{hs} + w_n^2} \tag{9}$$

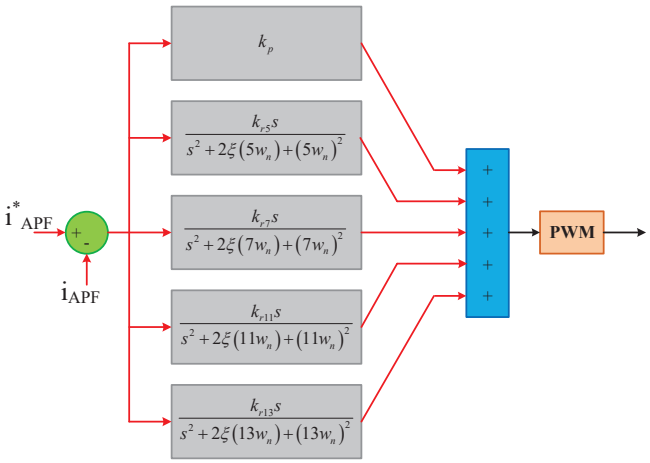

Fig. 3. The structure of multi-resonant controller.

Also, due to the gain k_p, the dynamic response is improved, yet the main problem regarding the SAPF is that different frequency must be compensated. As a result, several resonant controller should be used to provide zero steady state error at all of the frequencies. However, it is suggested that for lower frequencies, resonant controller is adopted while the gain k_p will be beneficial for high frequency components. It is mainly because with the increase of frequency, the harmonics amplitudes are usually decreased and also, the control system can response to finite dynamic with respect to the controller bandwidth. Since the most important and dominant harmonic components are 5th, 7th, 11th and 13th components in a three phase three wire systems, it is suggested that the multi-resonant controller tuned at these components is used to generate the harmonic components of SAPF. The structure of multi-resonant controller is depicted in fig. 3.

To avoid instability in resonant controller, a narrow bandwidth around central frequency usually adopted. This will reduce the controller gain which may result in steady state error at central frequency. However, with increase of K_R, the controller gain can be adjusted to reduce and eliminate the

error. The resonant bandwidth is selected about 10% of ω_n for 5th and 7th harmonic orders while it is decreased to about 5% for 11th and 13th harmonic orders.

IV. Simulation and Experimental Results

Simulation tests in MATLAB/SIMULINK supported with experimental results have been done to validate the proposed design procedure and control performance. The system parameters are listed in Table. 1. The DC-Link capacitor value and inductor filter are selected according to the proposed design procedure. The maximum DC voltage ripple is selected as 2% of nominal DC voltage and inductor current ripple is limited to 10% of the peak current value.

TABLE I. THE SYSTEM PARAMETERS

Grid Voltage (Vs)	70V(rms)
Grid Frequency	50Hz
Maximum SAPF current	20A
DC-Link Voltage	300V
Maximum DC voltage ripple	2% (6V)
Series Inductor Filter (Lf)	1mH
APF Input Capacitance (C)	2200uF
Switching Frequency	10kHz
Sampling Frequency	10kHz

It is worth to mention that almost all the implementation limitations such as sampling effect, control delay, deadtime and quantization effect are included in the simulations. To verify the effectiveness of the proposed design procedure and control method as well as to validate the simulation results, a prototype of three-phase APF is built, as shown in Fig. 4. The control system is implemented through DSP TMS28F335 from TI. The power semiconductors are SKM100GB12T4 with prototype driver, used as the main control board. In addition, three phase diode bridge rectifier with output resistance load is used as a non-linear load. On the other hand, LA55P LEM current sensors are used to measure the line, load and the SAPF currents. Also voltage transformers are utilized to sense the voltages.

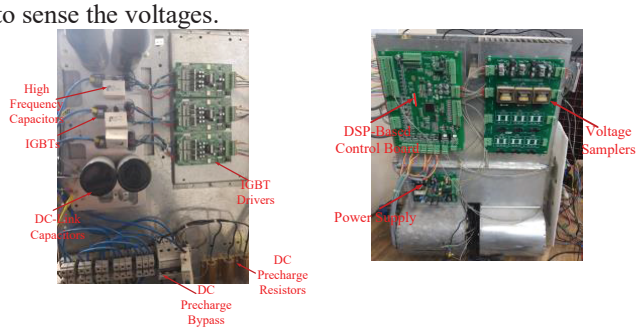

Fig. 4. The experimental setup of SAPF: a)Front view, b) back view.

Fig.5 shows the performance of SAPF implementing the proposed control method. It shows the phase 'A' of grid voltage, grid current, load current and SAPF current as well as the DC link voltage. Accordingly, the load currents are highly harmonic polluted but the SAPF effectively compensates the harmonics. In addition, synchronized grid voltage and current ensures complete reactive power compensation with unity power factor. Also, the DC-Link controller regulate and maintain the DC voltage at desired value with very low ripple (<0.25%). Based on this figure, it is seen that the injected current ripple is low compared to the peak grid current. The FFT analysis of the grid current without and with SAPF operation are depicted in Fig. 6. The grid current THD% is decreased from 21.59% to 1.68% in which dominants 5th and 7th harmonic orders are highly attenuated.

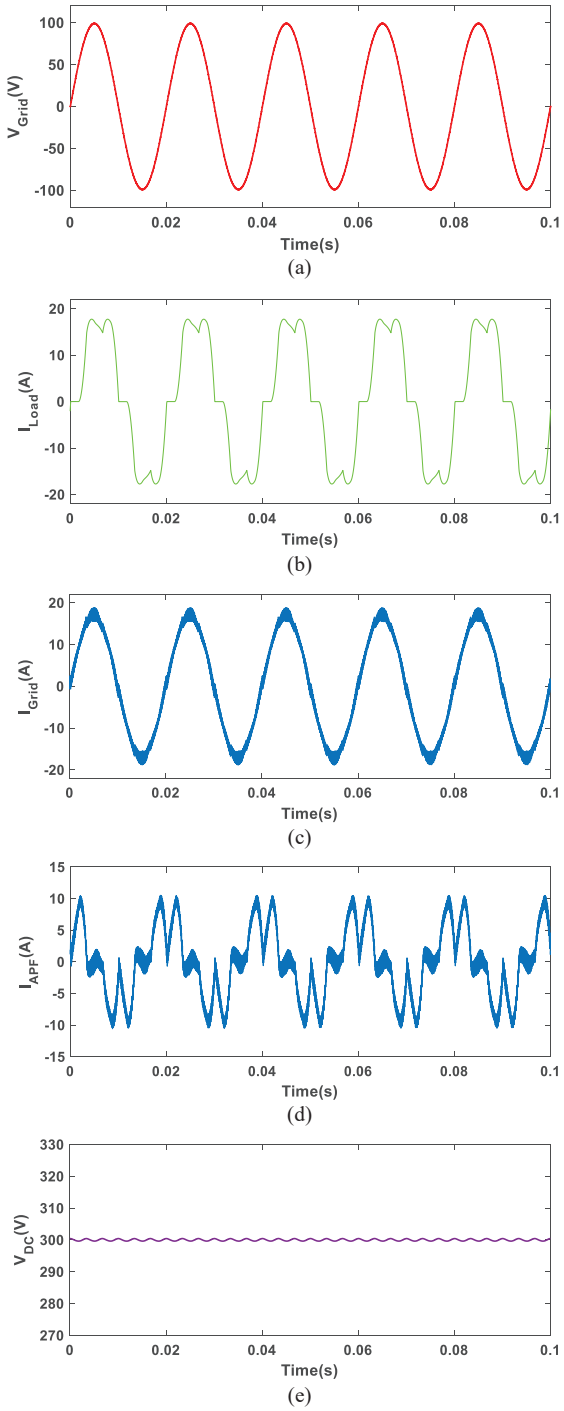

Fig. 5. Performance of SAPF with proposed control method: a) Grid voltage, b) Load Current, c) Grid current, d) APF current, e) DC link voltage.

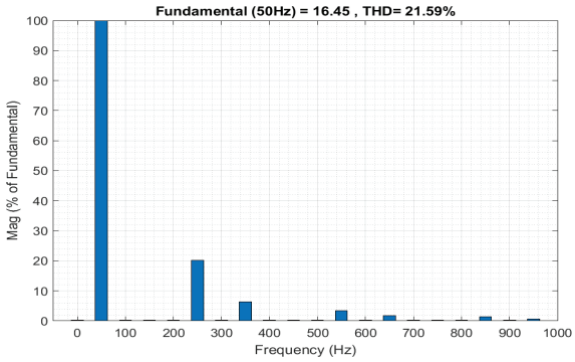

(a)

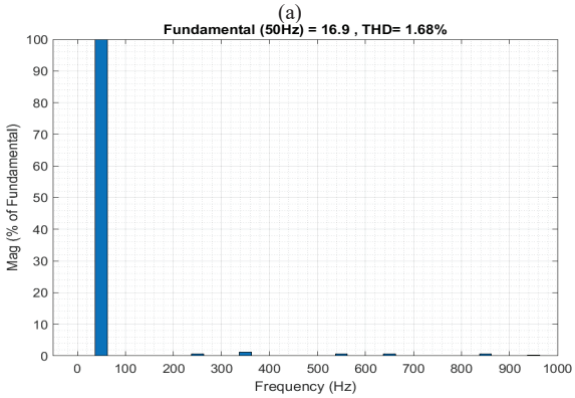

(b)

Fig. 6. FFT analysis of the grid current a) without and, b) with SAPF operation.

The experimental results under steady state condition are shown in Fig. 7. These include load, grid and SAPF currents in which the load harmonics are precisely detected and compensated by the SAPF. Also, the reactive power is fully compensated which results in synchronized sinusoidal current with the grid voltage. These results verify the performance of the proposed control method.

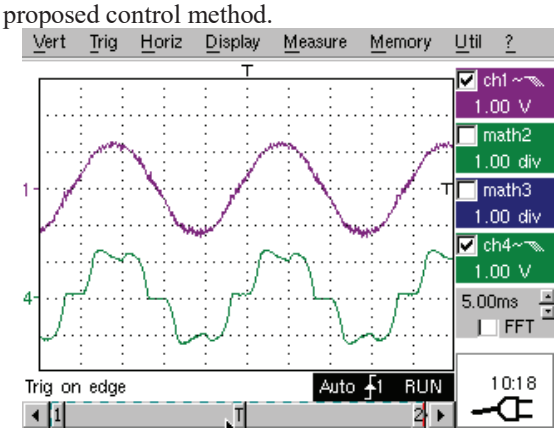

(a)

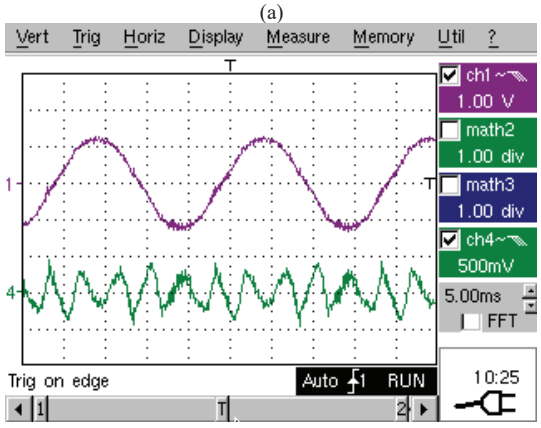

(b)

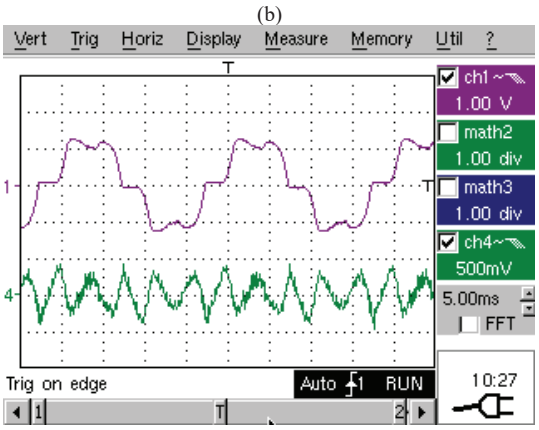

(c)

Fig. 7. The experimental results under steady state condition: a) ch1: grid current; ch2:load current (15A/div) ,b) ch1: grid current (15A/div); ch2: SAPF current (7.5A/div), c) ch1: load current (15A/div), ch2: (7.5A/div).

The harmonic components of the load and grid current after compensation with active and reactive powers are given in Fig. 8. It can be seen that THD% of grid current is improved by using proposed strategy in SAPF from 22% to 3%. This data is approved by FFT analyzer in Fig. 8 (c). Also, the power factor at grid side is improved and closed to 0.99. According to this fact that one step delay is eliminated from dead-beat controller, reference tracking is highly achieved which experimental results confirm this claim.

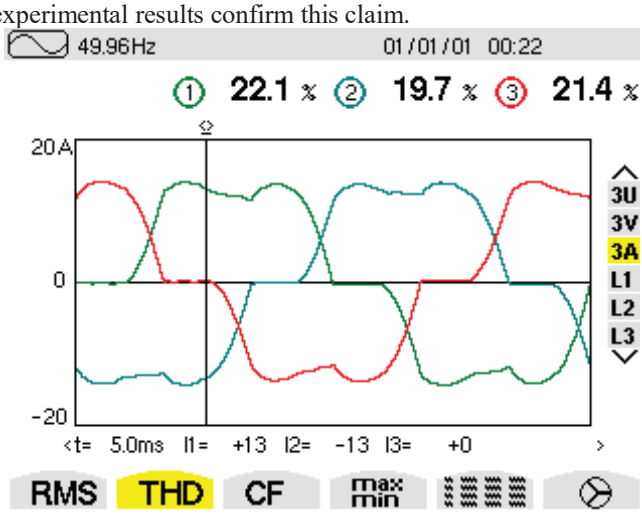

(a)

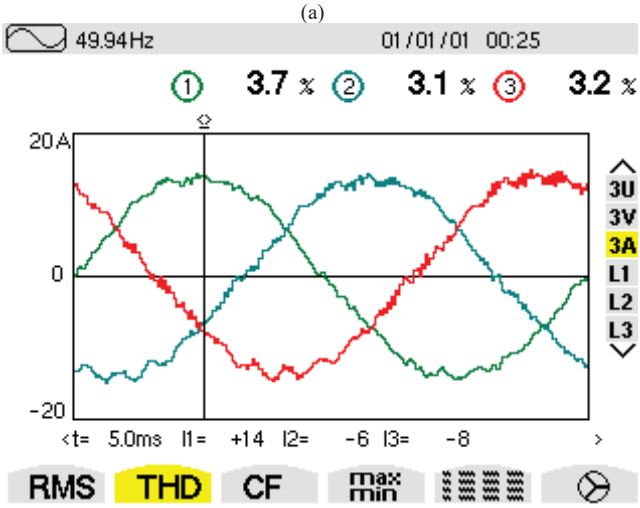

(b)

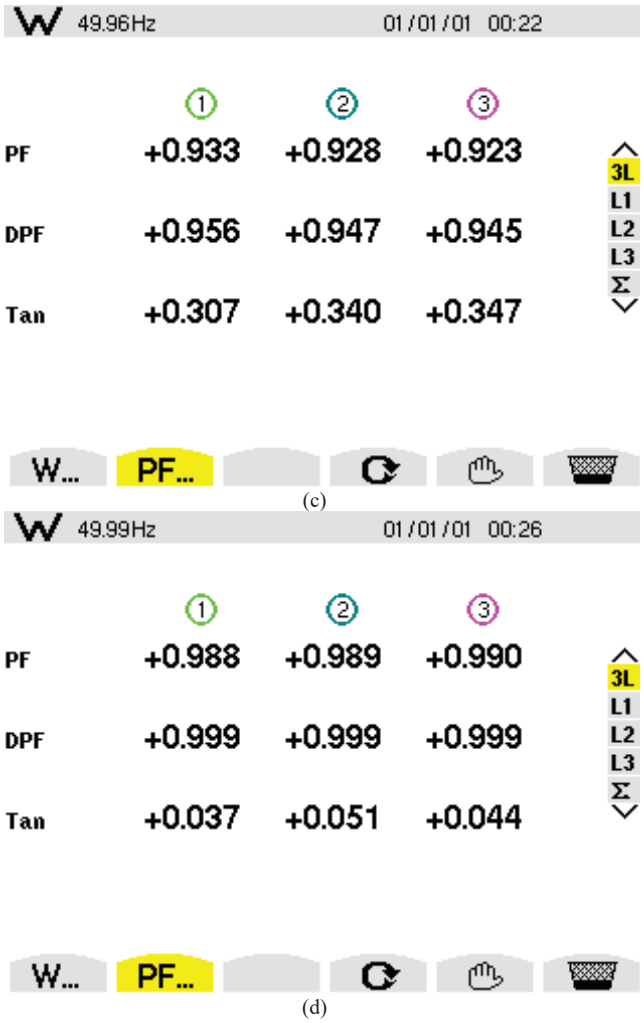

Fig. 8. The Harmonic and power factor analysis: a) the THD% of load currents, b) the THD% of grid currents with compensation, c) the FFT analysis of the load and grid currents, d) the power factor at grid side for phase 'A'.

V. Conclusion

Shunt active power filter (SAPF) is one the most efficient solutions to compensate both harmonic and reactive power imposed by the non-linear loads. However, lack of proper design of both passive elements and controller will decrease the overall performance of the SAPF. A logical procedure is adopted according to the PWM method to design the DC-link capacitor, whereas inductor filter is also designed properly. Also, an improved and well-performance multi-resonant controller is proposed to inject the current harmonic and reactive components. The general performance evaluation of the proposed procedure confirmed beneficial design and control where the grid current THD% is decreased to about 3.2% with unity power factor.

References

[1] J. Shair, H. Li, J. Hu, and X. Xie, "Power system stability issues, classifications and research prospects in the context of high-penetration of renewables and power electronics," *Renewable and Sustainable Energy Reviews,* vol. 145, p. 111111, 2021.

[2] G. Zhang, Z. Li, B. Zhang, and W. A. Halang, "Power electronics converters: Past, present and future," *Renewable and Sustainable Energy Reviews,* vol. 81, pp. 2028-2044, 2018.

[3] S. Ouchen, M. Benbouzid, F. Blaabjerg, A. Betka, and H. Steinhart, "Direct power control of shunt active power filter using space vector modulation based on supertwisting sliding mode control," *IEEE Journal of Emerging and Selected Topics in Power Electronics,* vol. 9, no. 3, pp. 3243-3253, 2020.

[4] S. A. Abrishamifar, M. Pichan, and M. Fazeli, "A 10KVA FPGA-based active power filter for battery charger applications," in *4th Annual International Power Electronics, Drive Systems and Technologies Conference*, 2013: IEEE, pp. 338-343.

[5] F. Z. Peng, "Harmonic sources and filtering approaches," *IEEE industry applications magazine,* vol. 7, no. 4, pp. 18-25, 2001.

[6] H. Akagi, "New trends in active filters for power conditioning," *IEEE transactions on industry applications,* vol. 32, no. 6, pp. 1312-1322, 1996.

[7] V. Gali, N. Gupta, and R. Gupta, "Mitigation of power quality problems using shunt active power filters: A comprehensive review," in *2017 12th IEEE Conference on Industrial Electronics and Applications (ICIEA)*, 2017: IEEE, pp. 1100-1105.

[8] M. Sarra, O. Aissa, and J.-P. Gaubert, "An investigation of solar active power filter based on direct power control for voltage quality and energy transfer in grid-tied photovoltaic system under unbalanced and distorted conditions," *Journal of Engineering Research,* vol. 9, no. 3B, 2021.

[9] Y. Zhang, Y. Peng, and C. Qu, "Model predictive control and direct power control for PWM rectifiers with active power ripple minimization," *IEEE Transactions on Industry Applications,* vol. 52, no. 6, pp. 4909-4918, 2016.

[10] S. Ouchen, M. Benbouzid, F. Blaabjerg, A. Betka, and H. Steinhart, "Direct power control of shunt active power filter using space vector modulation based on supertwisting sliding mode control," *IEEE Journal of Emerging and Selected Topics in Power Electronics,* vol. 9, no. 3, pp. 3243-3253, 2020.

[11] S. Ouchen, A. Betka, S. Abdeddaim, and A. Menadi, "Fuzzy-predictive direct power control implementation of a grid connected photovoltaic system, associated with an active power filter," *Energy conversion and management,* vol. 122, pp. 515-525, 2016.

[12] M. Malinowski, M. Jasinski, and M. P. Kazmierkowski, "Simple direct power control of three-phase PWM rectifier using space-vector modulation (DPC-SVM)," *IEEE Transactions on Industrial Electronics,* vol. 51, no. 2, pp. 447-454, 2004.

[13] M. Ferhat, L. Rahmani, and B. Babes, "DSP-based implementation of improved deadbeat control for three-phase shunt active power filters," *Journal of Power Electronics,* vol. 20, no. 1, pp. 188-197, 2020.

[14] L. Malesani, P. Mattavelli, and S. Buso, "Robust dead-beat current control for PWM rectifiers and active filters," in *Conference Record of 1998 IEEE Industry Applications Conference. Thirty-Third IAS Annual Meeting (Cat. No. 98CH36242)*, 1998, vol. 2: IEEE, pp. 1377-1384.

[15] V. Cardenas, N. Vazquez, C. Hernandez, and S. Horta, "Analysis and design of a three phase sliding mode controller for a shunt active power filter," in *30th Annual IEEE Power Electronics Specialists Conference. Record.(Cat. No. 99CH36321)*, 1999, vol. 1: IEEE, pp. 219-223.

[16] S. Hou and J. Fei, "A self-organizing global sliding mode control and its application to active power filter," *IEEE Transactions on Power Electronics,* vol. 35, no. 7, pp. 7640-7652, 2019.

[17] K. Antoniewicz, M. Jasinski, M. P. Kazmierkowski, and M. Malinowski, "Model predictive control for three-level four-leg flying capacitor converter operating as shunt active power filter," *IEEE transactions on industrial electronics,* vol. 63, no. 8, pp. 5255-5262, 2016.

[18] C. Lascu, L. Asiminoaei, I. Boldea, and F. Blaabjerg, "High performance current controller for selective harmonic compensation in active power filters," *IEEE Transactions on Power electronics,* vol. 22, no. 5, pp. 1826-1835, 2007.

[19] C. Xie, X. Zhao, K. Li, J. Zou, and J. M. Guerrero, "Multirate resonant controllers for grid-connected inverters with harmonic compensation function," *IEEE Transactions on Industrial Electronics,* vol. 66, no. 11, pp. 8981-8991, 2018.

[20] J. W. Kolar, S. D. Round, "Analytical calculation of the RMS current stress on the DC-link capacitor of voltage-PWM converter systems." *IEE Proceedings-Electric Power Applications*. Vol. 153, no. 4, pp. 535-43, Jul 2006.

[21] F. Krim, "Parameters estimation of shunt active filter for power quality improvement." *5th International Power Engineering and Optimization Conference*, pp. 306-311, Jun 2011.